Challenging Glass 6 - Conference on Architectural and Structural Applications of Glass
Louter, Bos, Belis, Veer, Nijsse (Eds.), Delft University of Technology, May 2018.

ISBN 978-94-6366-044-0, https://doi.org/10.7480/cgc.6.2161

Additive Manufacturing of Glass Components - Exploring the Potential of Glass Connections by Fused Deposition Modeling

Matthias Seel [a], Robert Akerboom [b], Ulrich Knaack [b], Matthias Oechsner [a], Peter Hof [a], Jens Schneider [b]
[a] *Center for Structural Materials, MPA-IfW, Technische Universität Darmstadt, Germany, seel@mpa-ifw.tu-darmstadt.de*
[b] *Institute of Structural Mechanics and Design, Technische Universität Darmstadt, Germany*

Glass is an indispensable material in the building industry. The combination of transparency, strength and durability makes it to an unparalleled and desirable material. The technology additive manufacturing (AM) has a potential in the building industry, based on a relatively small amount of repetitions of particular building components and the tendency of applying technology innovations for buildings. Therefore, there is an interest for additive manufacturing with glass. This paper presents and summarizes the results of the preliminary research regarding additive manufacturing of glass components for joining methods for flat glass structures. Different types of glass (borosilicate glass, quartz glass and soda lime silicate glass) are discussed. Experimental investigations of joints are intended to illustrate the performance and potential of AM glass components in case of structural use. Load bearing tests were carried out to quantify the strength and load bearing capacity level of an AM structural component. The thermal residual stresses were examined by photo-elastic tests with polarized lights and scattered light method. The investigations show in principle that load transfer via fused glass joints is possible. The performed research activity is a first step towards the Additive Manufacturing of glass structures on flat glass.

Keywords: Additive Manufacturing, Fused Deposition Modeling, Fused Glass Deposition Modeling, Fused Glass Joints

1. Introduction

Because of its unique combination of properties in terms of transparency, strength and durability, glass is an unparalleled and indispensable material for architects and engineers in the built environment. If we look at the developments in additive manufacturing, we can see a lot of potential for this technology in the building industry sector. Considering that production processes within this field are based on a relatively small amount of repetitions of particular building components and the tendency of using technological innovations for buildings, we see reasons to focus on additive manufacturing with glass (Knaack et al. 2010).

There is a great variety of additive processes that are common nowadays. What connects these techniques, such as Rapid Manufacturing, Rapid Tooling, Rapid Prototyping or, more generally, Additive Manufacturing (AM), is the fact that they are all based on 3D computer generated data as a framework for a manufacturing process. The desired components are digitally designed via a computer before this data is then converted in an applied computer language which commands the AM system to manufacture this specific component (Knaack et al. 2010; Hopkinson et al. 2006). Up until now, we don't see this technology used in the building industry to create end-use components. Instead, AM technology is mainly used for prototyping during design studies or for pre-cast-modeling. However, it seems that the focus of this technology is slowly heading towards manufacturing end-use components and because of the high potential, it is essential to find appropriate applications in the fields of architecture, building construction and façade engineering. If we think about the possibility of having single building components for the price of mass products, each field within the building industry has a potential market for this technology (Knaack et al. 2010, Hopkinson et al. 2006).

When we look at the most commonly used methods of additive manufacturing, we can distinguish the following four as dominant: 1. Fused Deposition Modeling (FDM), 2. 3D Printing (3DP), 3. Selective Laser Sintering (SLS) 4. Stereolithography (SLA). For all these methods can be said that they convert 3D data into physical models without extra tooling by solidifying layers of material on top of each other (Burmeister et al. 2005; Marchelli et al. 2010; Marchelli et al. 2011). Having a large pool of applicable materials enables us to dream of a wide range of fields for which products can be manufactured. Nowadays, all these methods of AM use either one or two materials at one time, and crossing these processes and thereby improving material properties seem to be the core of the matter.

Next to cost efficiency as an argument to justify the usage of AM technologies, a second and at least equally important argument can be given in terms of freedom of form. The freedom that is provided by these technologies in terms of form might include better structural and technical material or product properties, next to an increase of

individual design options. Moreover, building components with integrated functionality can be produced (Strauss 2010).

There are only few examples in which attempts have been made to use glass for additive manufacturing. An overview of additive manufacturing methods with glass is given in Seel et al. (2018). But what all these techniques have in common is the fact that they focus on individual glass components, printed in a single session on a non-glass base plate (Seel at el. 2018). If we look at the building industry however, it seems that there is a great potential in focusing on joining methods for flat glass structures. It is therefore that this paper presents the preliminary results of our research regarding fusing glass strings on a glass base plate (see Figure 1). These and subsequent investigations are the basis for additive manufacturing of glass components on flat glass plates.

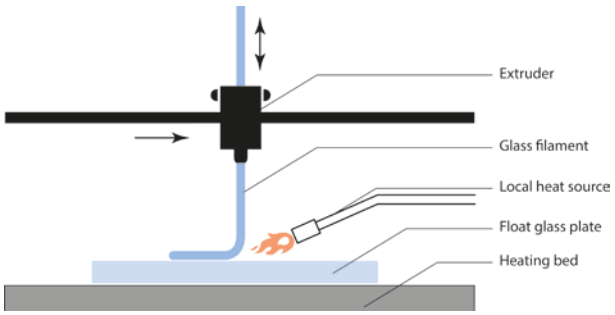

Fig. 1 Schematic representation of set-up for fusing glass connections on glass plates

2. Challenges during the manufacturing process and specimens

2.1. Challenges during the manufacturing process

The manufacturing process of fused glass specimens is sophisticated due to the high process temperatures, thermally induced residual stresses and the brittle material behaviour of glass. The process temperatures depend on the type of glass. The thermal and mechanical properties of soda lime silicate glass, borosilicate glass and quartz glass are listed in Table 1. Mainly soda lime silicate glass and borosilicate glass are used in the building sector. Quartz glass is not used due to high material costs and high processing temperatures. The thermal shock resistance depends on the strength and thermal expansion coefficient of the applied glass type. Lower thermal expansion coefficients lead to higher thermal shock resistance and better processability of the material glass, if the same strength is assumed. Undesirable cracks can occur during the manufacturing process, especially below the transformation temperature T_g, if the temperatures differ to much in the component. Therefore, borosilicate glass is better suited for additive manufacturing processes with glass than soda lime silicate glass. Specimens made of quartz glass are not manufactured due to the significantly higher process temperatures and a limited temperature processing window. For joining of different glass materials, the difference in thermal expansion coefficient should not exceed 0.3×10^{-6} K^{-1}.

Further studies on the feasibility of fused glass connections in the construction industry and the resulting challenges are listed in Rammig (2012).

Table 1: Thermal and mechanical properties of borosilicate, quartz and soda lime silicate glass

Property	Symbol	Borosilicate glass, Borofloat 33 (Schott Glas 2017)	Quartz glass (QSIL 2013)	Soda lime silicate glass (Öksoy et al. 1994)
Thermal expansion coefficient between 20 and 300 °C	$\alpha_{T,\,20/300}$ [K^{-1}]	3.3×10^{-6}	0.5×10^{-6}	(9×10^{-6} (DIN EN 572-1))
Max. usable temperature	T_{USE} [°C]	450 (long term) 500 (short term)	1100 (long term) 1300 (short term)	-
Thermal shock resistance	ΔT_{SR} [°K]	(125 …175 (GVB 2018))	-	(40 (DIN EN 572-1))
Transformation temperature	T_G [°C]	525	-	530
Strain point	T_{St} [°C]	518	1054	506
Annealing point	T_A [°C]	560	1204	550
Softening point	T_{So} [°C]	820	1730	725
Working point	T_W [°C]	1270	1700 … 2100	1030
Bending strength (non-toughened)	f_k [Nmm^{-2}]	25	68	(45 (DIN EN 572-1))

2.2. Production of specimens

The produced specimens for the tests were made manually. Figure 2 shows a manufactured point shaped glass joint. A torch, a heating plate, guide rails and insulation material were used to manufacture point shaped specimens. Guide rails were installed to minimize the unavoidable tolerances. In addition, fused rods were connected in line with glass plates. The manufacturing process and a line shaped specimen are shown in Figure 3. Glass plates and glass rods were used to produce the specimens. Soda lime silicate and borosilicate glass (Borofloat®33 (Schott 2017) and Duran® (Schott 2018)) were applied to manufacture the specimens. The used rods had a diameter of 2, 3, 4 or 5 mm. The thickness of the plates measured 2 and 3.4 mm. A heating plate was applied to preheat (approx. 300°C) the glass plates on the bottom surface (see Figure 1). A special torch for glass fusing was used to heat the joining area and the rest of the plate as well as the joining area of the glass rod. The temperatures in the joining area were not measured. It is supposed that these temperatures were within the working point temperatures of the used glass types (T_w > 1270 °C for borosilicate glass). A fused glass rod for the point shaped specimens was connected normal to and in the middle of the glass plate after a sufficient warming. The joint geometry was not perfectly rotationally symmetric due to the manual process and varies from specimen to specimen. Plate penetrations by the rods can occur during the joining process, since a not fully fused rod sinks slightly into the plate. The specimens were annealed in a kiln after the fusing process due to thermal residual stress. The annealing parameters were a maximum temperature of 540 °C for half an hour with a heating rate of 517 K h^{-1} and cooling rate of approx. 27 K h^{-1}. No visible deformations were occurred on the specimens due to the annealing.

Automation and optimization of the manufacturing process are the next steps in the development of additive manufacturing with glass. These activities are intended to produce reproducible and homogeneous samples. Figure 1 shows the schematic approach of a mechanized device which is able to create fused glass structures on glass plates.

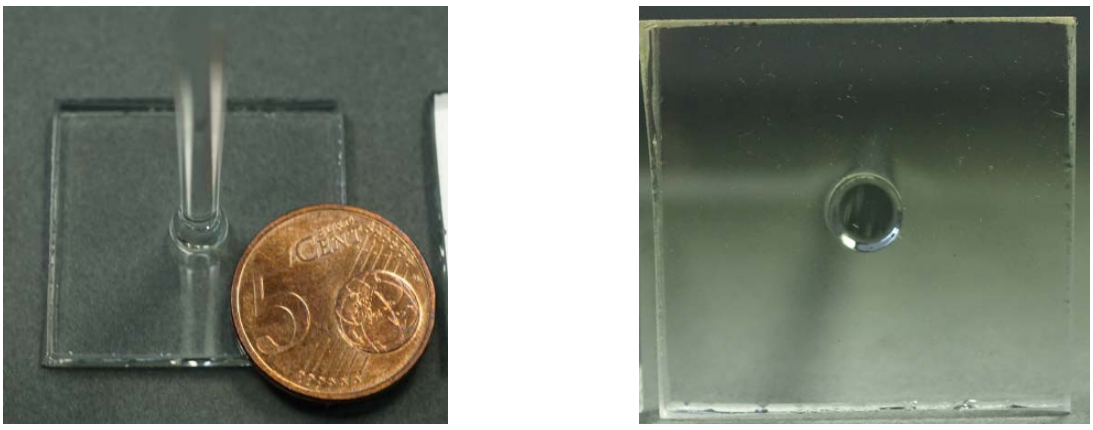

a) b)

Fig. 2 Point shaped specimens after manufacturing (borosilicate glass, rod diameter 3 mm, thickness glass plate 3.4 mm): a) perspective view, b) bottom view.

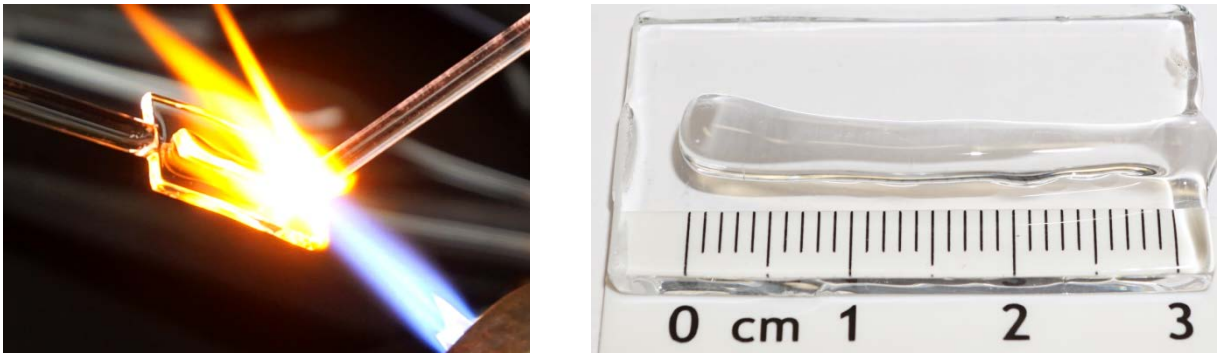

a) b)

Fig. 3 Line shaped glass joints (borosilicate glass): a) Manufacturing process; b) Perspective view

3. Investigations

The objectives of the investigations are the evaluation of residual stress and the load bearing capacity of the manufactures specimens.

3.1. Photo-elastic tests

Thermal residual stress can occur during the manufacturing process of the fused specimens due to the high process temperatures ($T > T_w$). Undesirable residual stress values lead to a decrease in the load bearing capacity and durability of a fused glass component. During the cooling phase, especially in the case of specimens made of soda lime silicate glass, fractures occurred frequently during manufacturing as a result of the induced residual stresses.

The investigation of residual stress is based on the optical effect of birefringence of glass. Stress free glass is optical isotropic. Optical anisotropy occurs if the glass component is under stress. The thermal residual stresses of the manufactured specimens are visualized by photo-elastic tests with polarized light (see Figure 4 and Figure 5). Figure 4 shows isochromatic lines (lines with same differences between principal stresses σ_{H1} and σ_{H2}) of a representative specimen before and after annealing. These isochromatic lines do not amount to the total residual stress values, but the stress distribution of the specimen can be derived from such an image.

a) b)

Fig. 4 Polarized image (circular) of sample P-BS34-BS3-t-B-8 (borosilicate glass for rod and plate): a) top view before annealing, b) top view after annealing

A complex measurement procedure with a polarimeter enables the determination of the total amount of stress values and the display of the stress distribution. An image of such a plot is illustrated in Figure 6. It should be noted that the measured values are integrated values via the glass thickness of the specimen. The absolute amount of residual stress ranges up to 20 N mm^{-2}. The images of the stress distribution before annealing illustrates that the higher stress values appear at the edge areas. An annealing of the specimens according to section 2.2 reduces the residual stress values significantly (see Figure 4).

Additional measurements of the residual stress on the plane surface of the fused specimens were carried out with the measuring device SCALP-05 (manufacturer GlassStress Ltd). The device could be applied in the flat area of the glass and not in the edge areas as a consequence of device geometry and the measuring technique. For all measuring points, three individual measurements are made. The results of this are the mean value of the three individual measurements. The measured residual stress values on the surface ranged from -3.5 to +9.0 N mm^{-2} (before annealing). Other investigations of the amount of residual stress in fused specimens showed similar results (Rammig 2016).

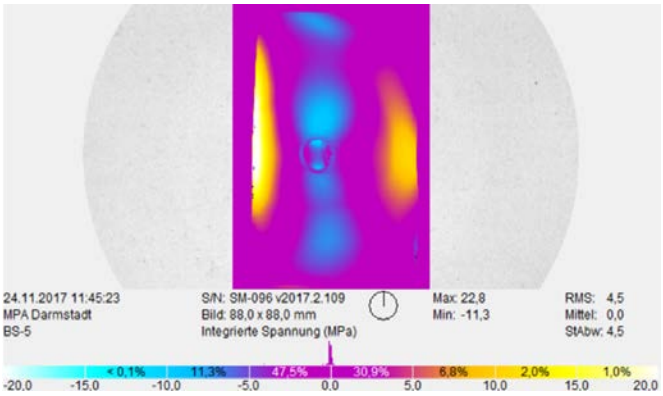

Fig. 5 Image of thermal residual stress of a sample (borosilicate glass for rod and plate) before annealing with measuring device StrainMatic M4/90 zoom (manufacturer ILIS)

3.2. Bending test

The load bearing capacity of the fused joint is the main objective of the investigations in order to evaluate the quality of this joining technique. For the determination of the load bearing capacity, bending tests were carried out on the point shaped specimens. A cantilever beam test with the maximum moment at the joining point between rod and plate is suitable as static system. The glass plate of the specimen was clamped at the lower part with plastics. The fused rod was loaded with a single load *F* at a defined distance. The load was applied to the rod via an eyelet, which was connected to the test machine via a chain. The chosen horizontal distance $L_{cant.}$ amount to 50 mm. The test set-up is shown in Figure 6.

The thickness of the plates for the point shaped specimens amount to 3.4 mm. The diameter of rod d_{rod} measured for series P-BS34-B3-t-B with 20 specimens 3 mm and for series P-BS34-B4-t-B with 17 specimens 4 mm. The bending tests were carried out with an universal testing machine (Instron, type 5882; 500 N load cell) at 23±2 °C with a humidity of 50±5 %.

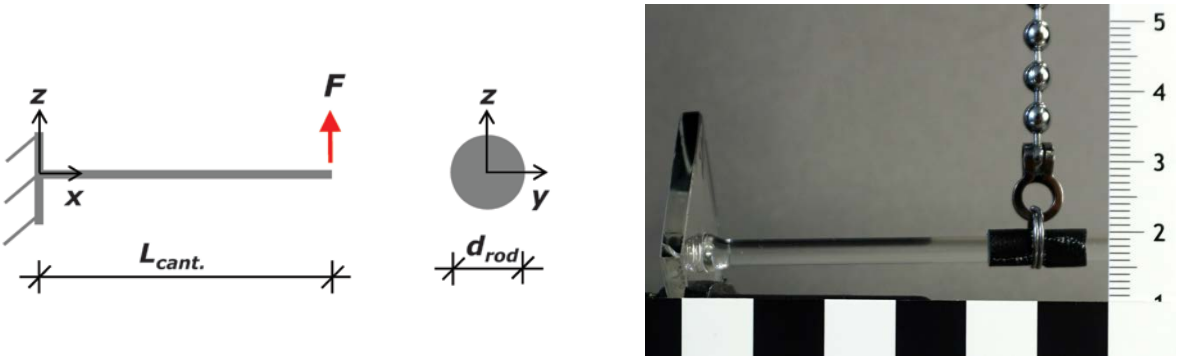

a) b)

Fig. 6 Test set-up of cantilever beam test: a) schematic image, b) view (without adhesive film)

Additional three-point bending tests were performed with single rods (series Ref-BS3-B and Ref-BS4-B) in order to compare the strength values with the determined strength values of the fused specimens. The diameters of rods correspond with those of the point shaped specimens (P-BS34-B3-t-B or P-BS34-B4-t-B). The length between the two support rolls measured 100 mm. The location of the single load was in the middle of the length between the two supports.

All specimens for the bending tests (cantilever and three-point bending) were made of borosilicate glass (Schott 2017; Schott 2018). Each load rate complied with the requirements of DIN 1288-3 (2000) of 2 N mm^{-2} s^{-1} at the maximum point of moment. This is the joining point of the point shaped specimens or the location of the single load for three-point bending test. An adhesive film was glued on each rod (bending pressure side) for identification of the failure origin.

The failure stress σ_f for the point shaped specimens was calculated in dependence of a section modulus for a circular cross-section by:

$$\sigma_f = \frac{32 \cdot F_u \cdot (L_{cant.} - x_{fo})}{\pi \cdot d_{rod}^3} \quad (1)$$

With

F_u = failure load

$L_{cant.}$ = length of cantilever

x_{fo} = origin of failure

d_{rod} = diameter of rod.

The approach of a circular cross-section and the usage of the section modulus are simplifications. The cross-sections of the joints are not perfectly regular and completely circular. The identification of fracture origin in the cross-section was in some cases ambiguous and unfeasible.

In addition to the mechanically based calculation of the failure stress σ_f according to Eq. (1), fractographic analysis of the fracture mirror can be used to determine the failure stress. The procedure of fractographic analysis for

ceramics and glass is proposed in ASTM C1678-10 (2015). The following empirically equation describes the relation between failure stress σ_f and the mirror radius r:

$$\sigma_f = \frac{A}{\sqrt{r}}. \tag{2}$$

The mirror constant A [N mm^{-2} m$^{1/2}$] depends on the type of glass. The inner mirror constant A_i (mirror-mist) for soda lime silicate glass is 1.8 (Mecholsky 1994) and for borosilicate glass 1.9 (Alarcón et al. 1994). Figure 7b) shows the fracture mirror of specimen P-BS34-BS3-t-B-11. The failure stress of P-BS34-BS3-t-B-11 with a measured inner radius r_i of 0.21 mm (average value) is 131 N mm^{-2}. According to Eq.(1), the failure stress amounts to 134 N mm^{-2}. In general, the method fractographic analysis is suitable for evaluation of failure stress if the fracture origin or mirror can be identified. Unfortunately, some fracture origins are not clear.

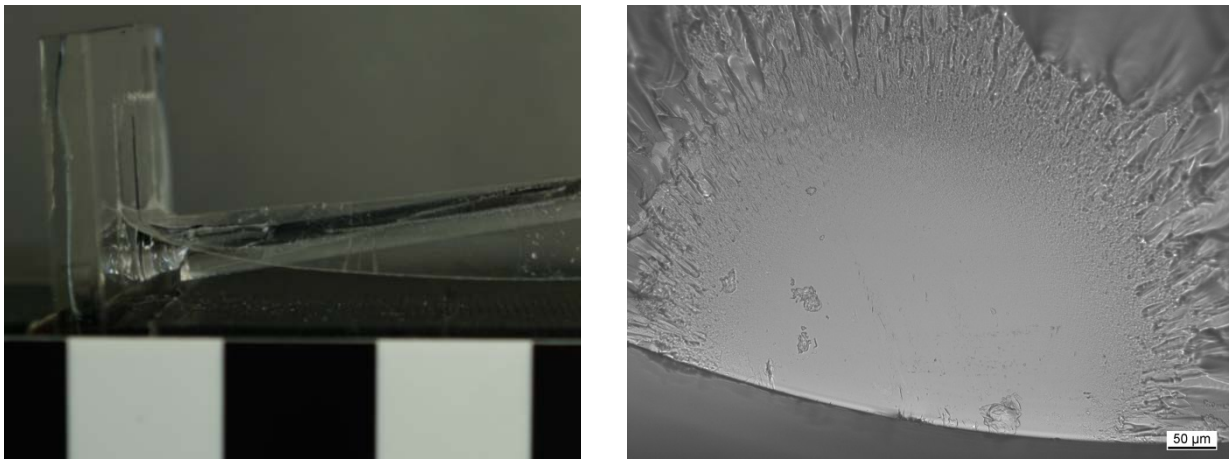

a) b)

Fig. 7 Specimen P-BS34-BS3-t-B-11 after bending test: a) view, b) microscopy image of fracture mirror and fracture origin

The focus of this investigation is the fundamental feasibility of this fused joining technology. The following evaluation is based on the failure stress values according to Eq. (1). The determination of the characteristic value of bending strength (5% fractile value, confidence level of 95%) for each series is done with the help of the lognormal distribution and a linear regression. The gradient of the regression line as well as the coefficient of variation represent the scattering of a series. The coefficient of determination R^2 indicates the prediction accuracy. For an accurate evaluation of characteristic failure stresses, a coefficient close to 1.0 is a desirable value.

The individual values of failure stress for series P-BS34-B3-t-B as well as Ref-BS3-B are shown in Figure 8 and for series P-BS34-B4-t-B as well as Ref-BS4-B in Figure 9. For comparison purposes, the respective series with the same rod diameter are plotted in one diagram. Furthermore, the data points of the fused specimens are marked according to the location of failure (joint or fracture). The test results for all series are summarized in Table 2.

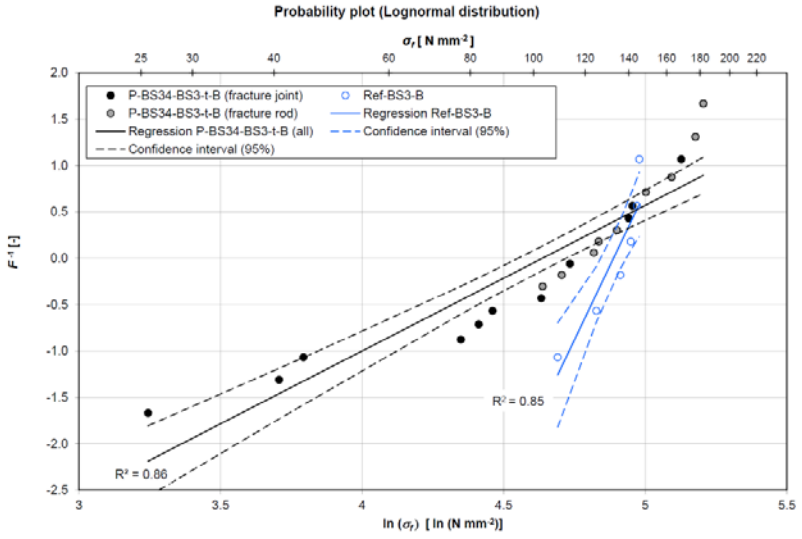

Fig. 8 Bending test - Probability plot (lognormal distribution) for series P-BS34-BS3-t-B (data points separated according to fracture joint and fracture rod) and Ref-BS4 with associated linear regression lines

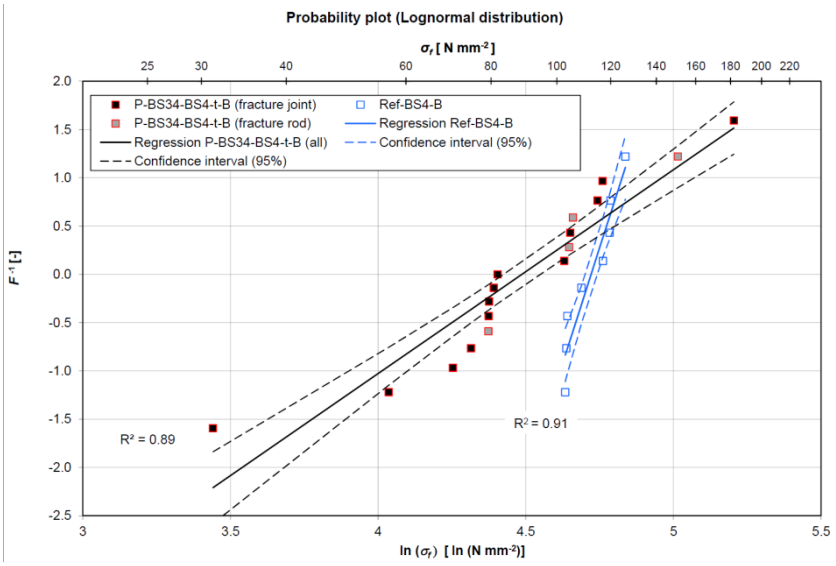

Fig. 9 Bending test - Probability plot (lognormal distribution) for series P-BS34-BS4-t-B (data points separated according to fracture joint and fracture rod) and Ref-BS4 with associated linear regression lines

The failure stress values for the fused series (P-BS34-B3-t-B and P-BS34-B4-t-B) ranges from 26 to 182 N mm^{-2} and for the reference series (Ref-BS3-B and Ref-BS4-B) from 103 to 145 N mm^{-2}. The mean value for series P-BS34-BS3-t-B is 113 N mm^{-2} and for P-BS34-BS4-t-B 95 N mm^{-2}. The mean values of the fused series are approx. 15 % lower than the respective values of the reference series. In comparison to the reference series (Ref-BS3-B and Ref-BS4-B), the failure stress values scatter in wide range (see Table 2). The maximum value of coefficient of variation amounts to 0.39. The high level of scattering can be a result of the manual process, the variations in the cross-sections and the remaining residual stress after the annealing. For bending tests on annealed soda lime silicate glass panes, the coefficient of variation of the failure stress is typically about 0.3 (Schneider et al. 2016). The characteristic values of series P-BS34-B3-t-B and P-BS34-B4-t-B amount to 35 % or 39 % of the corresponding reference values. The clear differences in the characteristic values between the fused and the reference series are a consequence of the high scattering.

The origin of failure for series P-BS34-B3-t-B is located nine times in the rod (see Figure 7a)) and eleven times at the joint. The failure occurs four times in the rod and fourteen times at the joint for series P-BS34-B4-t-B. Based on a comparison between the mean values of all fused specimens, the specimens with failure in the rod tend to show higher failure stress values than those with failure at the joint. Thus, the joining area is the weak point of the specimens.

The results of investigation demonstrate that a load transfer via a fuses manufactured glass joint is feasible in principle.

Table 2: Bending test – results for all series

Failure stress σ_f							
Series	Number of specimens	Amount of fracture origin (joint/rod)	Min. / max. value	Main Value	Standard deviation	Coefficient of variation	Characteristic value [a]
	[-]	[-]	[Nmm^{-2}]	[Nmm^{-2}]	[Nmm^{-2}]	[-]	[Nmm^{-2}]
P-BS34-BS3-t-B	20	11/9	25.6/ 182.2	114.6	45.1	0.39	28.7
Ref-BS3-B	6	-/6	108.9/ 145.3	133.4	14.1	0.11	81.9
P-BS34-BS4-t-B	17	13/4	31.2/ 182.1	95.0	35.0	0.37	34.7
Ref-BS4-B	8	-/8	102.9/ 126.1	112.6	9.1	0.08	88.9

Note: [a] 5%-fractile, lognormal distribution, 95% confidence level

4. Conclusion

This paper presents and summarizes the results of the preliminary research regarding additive manufacturing of glass components for joining methods on flat glass plates. The aim of the investigations was the manufacturing of fused glass joints and the evaluation of the load bearing capacity of the produces specimens.

As a consequence of the high process temperatures, the occurrence of residual stress and the brittle material behavior of glass, the manufacturing of fused glass structures is sophisticated. The investigations demonstrate that the manufacturing of fused glass components on flat glass plates is feasible. Line and point shaped specimens were manufactured. Borosilicate glass is better suited for additive manufacturing processes with glass than soda lime silicate glass due to the lower thermal expansion properties of borosilicate glass.

The residual stresses caused by the manufacturing were visualized and quantified by means of photo-elastic tests. Additional non-destructive investigations (3D computer tomography) and microscopy analysis in combination with energy dispersive X-ray spectroscopy (EDX) of the specimens are presented in Seel et al. (2018). The bending tests show that load transfer via fused glass joints on glass plates is feasible.

Further steps are planned to minimize production tolerances and to optimize the manufacturing process. The aim is the production of reproducible and homogeneous specimens. In addition to the bending tests, supplemental investigations (hardness tests and fractography) are planned to analyse the causes of failure and strength at the interface between the plate and fused material (Kerkhof 1970). Issues of thermal shock resistance and post-breakage behaviour have to be analysed and considered for a practical realization in an architectural application.

The performed studies are a first step towards the Additive Manufacturing of glass structures on flat glass plates.

Acknowledgements

The authors gratefully acknowledge the company Schott for material support and the company ILIS GmbH for photo-elastic measurements of manufactured samples. Special thanks go to Mr. Wittmann (Department of Chemistry, TU Darmstadt) for his support in manufacturing and his exchange of experience.

References

Alarcón, O.E., Medrano, R.E., Gillis, P. P.: Fracture of Glass in Tensile and Bending Tests. Metallurgical and Materials Transactions A, Vol. 25A, 961-967 (1994).
ASTM C 1678-10: Standard Practice for Fractographic Analysis of Fracture Mirror Sizes in Ceramics and Glasses. (2015).
Burmeister, K., Kremp, S.: Vom Personal Computer zum Personal Fabricator. Murmann Verlag, Hamburg (2005).
DIN EN 572-1: Glas im Bauwesen - Basiserzeugnisse aus Kalk-Natronsilicatglas - Teil 1: Definitionen und allgemeine physikalische und mechanische Eigenschaften. Beuth Verlag GmbH, Berlin (2016).
DIN EN 1288-3: Glas im Bauwesen - Bestimmung der Biegefestigkeit von Glas - Teil 3: Prüfung von Proben bei zweiseitiger Auflagerung (Vierschneiden-Verfahren). Beuth Verlag GmbH, Berlin (2000).
GVB: New Boroplate - Planes gefloatetes Borosilikatglas. Datasheet, GVB GmbH-Solutions in Glass. www.g-v-b.de/borosilikatglass__313.php. accessed 19 January 2018.
Hopkinson, N., Hague, R., Dickens, P.: Rapid Manufacturing - An Industrial Revolution for the Digital Age. John Wiley and Sons, Chichester (2006).
Kerkhof, F.: Bruchvorgänge im Glas. Verlag der deutschen glastechnischen Gesellschaft, Frankfurt am Main (1970).
Knaack, U., Klein, T., Bilow,M.: imagine 04 – Rapids. 010 Verlag, Rotterdam (2010).
Marchelli, G., Storti, D., Ganter, M., Prabhakar, R.: An Introduction to 3D Glass Printing. Proceedings of the International Solid Freeform Fabrication Symposium - An Additive Manufacturing Conference, 95-107 (2010).
Marchelli, G., Prabhakar, R., Storti, D., Ganter, M.: The guide to Glass 3D printing: developments, methods, diagnostics and results. Rapid Prototyping Journal, Volume 17 Issue 3, 187-194 (2011).
Mecholsky, J.J.: Quantitative Fractographic Analysis of Fracture Origins in Glass. Fractography of Glass, 37-172 (1994).
Öksoy, D., Pye, L.D., Boulos, E.N.: Statistical analysis of viscositycomposition data in glassmaking. Glastechnische Berichte Bd. 67.7, 189–195 (1994).
QSIL: Materialspezifikation Quarzglas ilmsil PN. Datasheet. QSIL GmbH (2013).
Rammig, L.: Direct Glass Fabrication – New applications of glass with additive processes. Challenging Glass 3, Delft, 315-321 (2012).
Rammig, L.: Residual Stress in Glass Components. Challenging Glass 5, Gent, 305-314 (2016).
Schneider, J., Kuntsche, J., Schula, S., Schneider, F., Wörner, H.-D.: Glasbau Grundlagen, Berechnung, Konstruktion. Springer Vieweg, Berlin (2016).
Schiffner, U: Fügen von Glas. Hüttentechnische Vereinigung der Deutschen Glasindustrie. Frankfurt/Main (1995).
Schott: Borofloat®33. Datasheet. Schott Glas. http://www.schott.com/borofloat/german/download/index.html, Accessed: 20 October 2017.
Schott: Duran®. Datasheet. Schott Glas. http://www.schott.com/d/tubing/6779e411-7f0c-4a51-ae99-6e88d41abf80/schott-tubing-datasheet-duran-german.pdf. accessed 19 January 2018.
Seel, M., Akerboom, R., Knaack, U., Oechsner, M., Hof, P., Schneider, J.: Fused glass deposition modelling for applications in the built environment. Materialwissenschaft und Werkstofftechnik, submitted (2018).
Strauss, H.: Funktionales Konstruieren – Rapid Technologien für Architektur und Baukonstruktion. RTejournal – Forum für Rapid Technologie, Vol. 7. (2010)